

# High Performance Adaptive Attitude Control of a Quadrotor

Dinu Mihailescu-Stoica<sup>1</sup>, Raul Acuna<sup>1</sup> and Jürgen Adamy<sup>1</sup>

**Abstract**—This paper introduces a quaternion based attitude controller, by augmenting a novel baseline controller with model reference adaptive control techniques (MRAC). In contrast to existing designs, the baseline controller makes use of the quaternion logarithm and the standard bi-invariant distance on  $SO(3)$ . The adaptation restores the behavior of a time dependent reference model in case of model discrepancies. Moreover, we make use of the fact that the parameters, characterizing the gyroscopic coupling term of a rigid tumbling body, are naturally bounded to some predefined manifold and incorporate this information in our adaptive design. Altogether, the proposed design enables aggressive, high bandwidth acrobatic flight maneuvers over the whole attitude range without singularities, even in the presence of parametric uncertainties. Experimental results on our custom quadrotor platform validate the performance and robustness of the proposed attitude controller.

## NOTATION

In the following, vectors are depicted as small lower case, bold symbols like  $\mathbf{a}$ ,  $\boldsymbol{\alpha}$ , etc. and matrices and tensors from order two as capital bold symbols, e.g.,  $\mathbf{A}$ ,  $\mathbf{B}$ .

$\mathcal{B}$	Body reference frame
$\mathcal{I}$	Inertial reference frame
$\mathcal{C}$	Command reference frame
$\mathbf{a}$	A vector in general vector notation, i.e. without declaration of a component frame
$\mathcal{X}(\cdot)$	Vector, Tensor in $\mathcal{X}$ -frame components
$[\cdot]_{\times} : \mathbb{R}^3 \rightarrow \mathfrak{so}(3)$	Skew-symmetric matrix satisfying $\mathbf{a} \times \mathbf{b} = [\mathbf{a}]_{\times} \mathbf{b}$
$(\dot{\cdot}) = \frac{\partial}{\partial t}(\cdot)$	Component wise time derivative
$\frac{d}{dt}$	Time derivative with respect to $\mathcal{X}$ -frame
$\boldsymbol{\omega}_{\mathcal{X}\mathcal{Y}}$	Angular velocity of $\mathcal{X}$ -frame w.r.t. $\mathcal{Y}$ -frame
$\boldsymbol{\omega}_{\mathcal{X}}$	Angular velocity of $\mathcal{X}$ -frame w.r.t. $\mathcal{I}$ -frame
$\boldsymbol{\omega}_{\mathcal{B}}$ , $\boldsymbol{\omega}_{\mathcal{B}}$	Angular velocity of $\mathcal{B}$ -frame w.r.t to $\mathcal{I}$ -frame
$\mathbf{R}_{\mathcal{Y}\mathcal{X}} \in SO(3)$	Rotation matrix from $\mathcal{X}$ - to $\mathcal{Y}$ -frame
$\mathbf{q}_{\mathcal{Y}\mathcal{X}}$	Unit quaternion describing the rotation from $\mathcal{X}$ - to $\mathcal{Y}$ -frame
$\mathbf{q}$	Unit quaternion describing the rotation from $\mathcal{B}$ - to $\mathcal{I}$ -frame
$\mathbf{q}_c$	Desired unit quaternion describing the rotation from $\mathcal{C}$ - to $\mathcal{I}$ -frame
$\epsilon$	Pure imaginary vector part of a quaternion
$\mathbf{I}$	Identity matrix of appropriate dimensions
$\mathbf{0}$	Zero matrix of appropriate dimensions
$(\cdot)_D$	Nominal design values used for the baseline control design

## I. INTRODUCTION

Unmanned aerial vehicles and especially multicopter systems have encountered a tremendous amount of interest in

the control and robotics research community during the last two decades. This focus certainly is based on the cost-efficient manufacturing leading to a wide commercialization, delivering easy to use, ready to flight systems for both consumer and professional applications.

While initially attitude stabilization of the linearized system around a hover state with linear PID or LQR controllers [4] was one of the main topics in the literature, this focus rapidly changed to nonlinear controllers, enabling trajectory tracking beyond the range of valid linearization.

Meanwhile, a lot of nonlinear controller architectures have been proposed for both attitude and position control in the literature consisting of exact input/output linearization [21], backstepping [18], sliding mode [15] or nonlinear PD<sup>2</sup> control [25], just to name a few. Most contributions dealing with adaptive control of multicopter, however, propose controllers based upon linearized attitude kinematics [6], [24], which leads to three decoupled double integrators for the attitude dynamics. Another approach is to use cascaded loops for attitude and angular rates with a full adaptive inner loop control [1], which however requires bandwidth separation. In both cases, the nonlinear system is forced to follow a linear reference model and thus the performance is limited to the achievable by linear dynamics. Full nonlinear adaptive controllers, like the one in [16], appear more seldom and do not suffer from the restrictions of linearization. In contrast, [2] proposes an adaptive augmentation of a nonlinear baseline controller, which shall restore the nominal, nonlinear closed loop behavior. This approach leads in general to more robust and yet performant controllers than the full adaptive ones [20]. A remarkable amount of publications dealing with quaternion based attitude stabilization in general use, for example, the euclidean distance in  $\mathbb{R}^4$  or the norm of the pure quaternion in order to synthesize a Control Lyapunov Function for control design, e.g. [2], [12], [13]. However, this leads to a distorted distance on the group of rotation matrices. Another approach is given by geometric controllers on  $SO(3)$  which respect the underlying topology of the nonlinear system. These controllers are based on a Direction Cosine Matrix (DCM) description of the rigid body dynamics, c.f. [16], [27]. While singularities and ambiguities are omitted, calculations are more costly, when compared to other attitude representations like quaternions or Modified Rodriguez Parameters.

The aim of the present paper is to combine the methods of geometric control design in a quaternion formulation, with modern adaptive control in order to achieve fast trajectory tracking and adaptation. For this scope, we design a novel geometric controller for the nominal system which uses

<sup>1</sup>Dinu Mihailescu-Stoica, Raul Acuna and Jürgen Adamy are with the Control Methods and Robotics Lab, Technische Universität Darmstadt, Darmstadt 64283, Germany. {dinu.mihailescu-stoica, racuna, adamy}@rmr.tu-darmstadt.de

the geodesic bi-invariant distance on  $SO(3)$ . This baseline controller is augmented with an indirect model reference adaptive control (MRAC), following a time variant reference model. The plant is therefore forced to follow the nominal nonlinear design plant despite parametric uncertainties. Furthermore the estimated parameters by the MRAC, representing the gyroscopic cross coupling, are bounded to physically plausible values. As a result, cumbersome identification procedures for the physical parameters are omitted. Especially when the system is subject to payload changes, controller re-tuning is usually necessary to restore the original flight performance.

The ability of the attitude controller to perform aggressive maneuvers is not only for its own sake but as well an enabling capability in order to perform more complex tasks, like the one in [17]. Finally, we would like to emphasize, that the attitude control problem arises in many different settings and the methods presented herein are by no means restricted to quadrotor systems.

The remainder of the present article is organized as follows. Section 2 recapitulates the quaternion-based attitude representation and introduces the system model of the uncontrolled quadrotor. Subsequent the controller is developed in Section 3. A trajectory generator is introduced and the tracking error equations are established. Based on the error dynamics a nominal geometric attitude controller for the unperturbed system is developed which is augmented by an adaptive controller to cancel out the uncertainties. Finally we validate the approach by real flight tests in Section 4.

## II. MODELING OF THE QUADROTOR DYNAMICS

### A. Attitude Description and Rigid Body Dynamics

Consider a body fixed, principal coordinate frame  $\mathcal{B}$  with the orthonormal, right-handed basis  $\{\mathbf{b}_x, \mathbf{b}_y, \mathbf{b}_z\}$  and an inertial North-East-Down (NED) frame  $\mathcal{I}$  with the basis  $\{\mathbf{e}_x, \mathbf{e}_y, \mathbf{e}_z\}$ , c.f. Figure 1. Rigid body rotations in the three dimensional space can be represented without singularity by unit quaternions  $\mathbf{q} = (q_0, \boldsymbol{\epsilon}^\top)^\top \in S^3 \subset \mathbb{R}^4$ , which describe a vector rotation from the  $\mathcal{B}$ -frame to the  $\mathcal{I}$ -frame. The map  $\rho : S^3 \rightarrow SO(3)$  denotes the corresponding rotation matrix<sup>1</sup> to a given unit quaternion:

$$\rho(\mathbf{q}) = \mathbf{I} + 2q_0[\boldsymbol{\epsilon}]_{\times} + 2[\boldsymbol{\epsilon}]_{\times}^2. \quad (1)$$

Note that  $\rho(\mathbf{q})$  is a group homomorphism, satisfying  $\rho(\mathbf{q} \otimes \mathbf{p}) = \rho(\mathbf{q})\rho(\mathbf{p})$ , for two given unit quaternions  $\mathbf{p}$  and  $\mathbf{q}$ , with  $\otimes$  being the quaternion product which is defined as:

$$\mathbf{q} \otimes \mathbf{p} = \begin{pmatrix} q_0 \\ \boldsymbol{\epsilon}_q \end{pmatrix} \otimes \begin{pmatrix} p_0 \\ \boldsymbol{\epsilon}_p \end{pmatrix} = \begin{pmatrix} q_0 p_0 - \boldsymbol{\epsilon}_q^\top \boldsymbol{\epsilon}_p \\ q_0 \boldsymbol{\epsilon}_p + p_0 \boldsymbol{\epsilon}_q + \boldsymbol{\epsilon}_q \times \boldsymbol{\epsilon}_p \end{pmatrix}. \quad (2)$$

The multiplicative identity quaternion therefore is  $\mathbf{q}_{\text{id}} = (1, 0, 0, 0)^\top$ . The complex conjugate of a quaternion is given by  $\bar{\mathbf{q}} = (q_0, -\boldsymbol{\epsilon}^\top)^\top$  and the inverse of a quaternion follows to be  $\mathbf{q}^{-1} = \bar{\mathbf{q}}/|\mathbf{q}|^2$ , which is equivalent to its complex

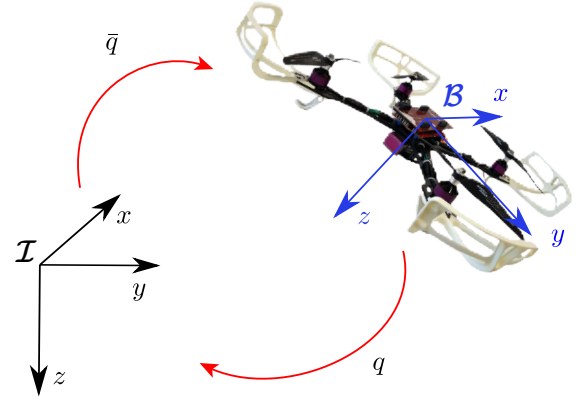


Fig. 1. Quadrotor and coordinate frames.

conjugate for a unit length quaternion. A rotation of a vector by a quaternion is obtained by

$$\boldsymbol{\epsilon}({}^X \mathbf{v}) = \mathbf{q} \otimes \boldsymbol{\epsilon}({}^Y \mathbf{v}) \otimes \bar{\mathbf{q}} =: \text{Ad}_{\mathbf{q}} \boldsymbol{\epsilon}({}^Y \mathbf{v}), \quad (3)$$

where  $\boldsymbol{\epsilon}(\mathbf{v}) = (0, \mathbf{v}^\top)^\top$ . However, the map (1) is not injective as a unit quaternion  $\mathbf{q}$  and its antipodal  $-\mathbf{q}$  describe the same rotation, see (3). Therefore one may define the set valued function  $\mu : SO(3) \rightrightarrows S^3$

$$\mu(\mathbf{R}) := \text{preim}_{\rho}(\mathbf{R}) = \{\mathbf{q}, -\mathbf{q}\}. \quad (4)$$

This fact is known as the double coverage of  $SO(3)$ . A more detailed analysis of  $\mathbf{q}$  and  $-\mathbf{q}$  reveals that the two quaternions represent the short and long way rotation depending on the sign of  $q_0$ . Therefore we define the  $(\cdot)^+$  operator given by

$$\mathbf{q}^+ = \begin{cases} \mathbf{q} & , q_0 \geq 0 \\ -\mathbf{q} & , q_0 < 0, \end{cases} \quad (5)$$

which returns the short rotation quaternion with an angle smaller or equal to  $\pi$ . The principal rotation angle  $\alpha$  of a quaternion rotation is obtained by the logarithm  $\log(\mathbf{q}) = \alpha/2 \cdot (0, \mathbf{n}^\top)^\top$ , where  $\mathbf{n}$  is the eigenaxis of the rotation with unit length and therefore  $\alpha^2 = 4 \cdot \langle \log(\mathbf{q}), \log(\mathbf{q}) \rangle$ , where  $\langle \cdot, \cdot \rangle$  is the standard inner product in  $\mathbb{R}^4$ . Notice, that the logarithm of quaternions is well defined for all quaternions with unit length  $\log : S^3 \rightarrow \{(0, \mathbf{v}^\top)^\top \mid \mathbf{v} \in \mathbb{R}^3\}$ , especially  $\log \pm \mathbf{q}_{\text{id}} = \mathbf{0}$  holds. See the Appendix for calculation of the quaternion logarithm. Further, the inner product of the logarithm gives the geodesic distance on  $SO(3)$  [8] by

$$d(\rho(\mathbf{q})) = \|\log \rho(\mathbf{q})\| = 2 \langle \log(\mathbf{q}^+), \log(\mathbf{q}^+) \rangle^{\frac{1}{2}} =: \|\mathbf{q}\|_{SO(3)} \in [0, \pi], \quad (6)$$

which we will make use of during the controller synthesis via Lyapunov methods. For ease of notation, let us additionally define the function  $\log_v \mathbf{q} := \alpha/2 \cdot \mathbf{n}$ , which directly maps into  $\mathbb{R}^3$  instead of  $\mathbb{R}^4$ .

The kinematics of a rotating rigid body can be given as:

$$\dot{\mathbf{q}} = \frac{1}{2} \mathbf{q} \otimes \begin{pmatrix} 0 \\ \mathbf{B} \boldsymbol{\omega}_{\mathcal{B}\mathcal{I}} \end{pmatrix} = \frac{1}{2} \begin{pmatrix} 0 \\ \mathcal{I} \boldsymbol{\omega}_{\mathcal{B}\mathcal{I}} \end{pmatrix} \otimes \mathbf{q}. \quad (7)$$

<sup>1</sup>A rotation matrix is part of the special orthogonal group  $SO(3) := \{\mathbf{R} \in \mathbb{R}^{3 \times 3} \mid \mathbf{R}^\top \mathbf{R} = \mathbf{I}, \det \mathbf{R} = 1\}$ .

Due to the pure kinematic relationship, no parametric uncertainty acts on this part of the quadrotor dynamics. It can be shown, either by using the derivative of the angle-axis representation [23] or by general Lie group theory [5], that the derivative of the quadratic distance function  $d$  equals

$$\frac{1}{2} \frac{d}{dt} \|\mathbf{q}\|_{\mathfrak{so}(3)}^2 = 2 \frac{d}{dt} \langle \log \mathbf{q}^+, \log \mathbf{q}^+ \rangle = {}^B \boldsymbol{\omega}^\top \log_v \mathbf{q}^+ \quad (8)$$

with the angular velocity of the body expressed in  $\mathcal{B}$ -frame components  ${}^B \boldsymbol{\omega} \in \mathbb{R}^3 \cong \mathfrak{so}(3)$ .

For vector differentiation we will use the transport theorem from classical mechanics [23], which connects the time derivatives of a vector w.r.t. two arbitrary reference frames  $\mathcal{X}$  and  $\mathcal{Y}$ , which rotate relative to each other:

$${}^{\mathcal{X}} \frac{d}{dt} \mathbf{v} = {}^{\mathcal{Y}} \frac{d}{dt} \mathbf{v} + \boldsymbol{\omega}_{\mathcal{Y}\mathcal{X}} \times \mathbf{v}. \quad (9)$$

The angular acceleration therefore follows from the kinetics given by Euler's formula:

$${}^B \mathbf{J} \dot{\boldsymbol{\omega}}_{BI} = -\boldsymbol{\omega}_{BI} \times {}^B \mathbf{J} \boldsymbol{\omega}_{BI} + \boldsymbol{\tau}_{ext} \quad (10)$$

Herein  $\boldsymbol{\tau}_{ext}$  is the sum of external moments which act on the quadrotor and can be further split into  $\boldsymbol{\tau}_{ext} = \boldsymbol{\tau}_c + \boldsymbol{\tau}_{prop} + \boldsymbol{\tau}_d$ . The gyroscopic torques due to the propeller rotation are denoted by  $\boldsymbol{\tau}_{prop}$ ,  $\boldsymbol{\tau}_c$  is the commanded torque of the control system and  $\boldsymbol{\tau}_d$  is some unknown disturbance. However, as the rotors have pairwise opposite directions of rotation, we will neglect the gyroscopic term for the scope of controller design, i.e.  $\boldsymbol{\tau}_{ext} \approx \boldsymbol{\tau}_c + \boldsymbol{\tau}_d$ .

### B. Thrust and Motor-Dynamics

Each rotor  $i$  generates a thrust, whose magnitude is proportional to its squared angular velocity, i.e.  $f_i = c_f \omega_{R_i}^2$  and which is pointing in direction of  $-\mathbf{b}_z$ . Additionally, a moment around the rotor axis originates due to friction, which opposes the sense of rotation. This moment is proportional to the generated force by  $\tau_i = -\text{sign}(\omega_{R_i}) c_m f_i$ . The affine relation  $\omega_{R_i}^{tar} \approx c_{u_1} u_i + c_{u_0}$  relates the target angular velocity to the input of the brush-less motor driver, with the two empirically determined constants  $c_{u_1}$  and  $c_{u_0}$ . The closed loop dynamics of each motor in conjunction with its motor driver can be described by a nonlinear PT1-like system, consisting a time constant, that is both dependent on the set-point  $\omega_{R_i}$  and additionally differs if the rotor is accelerating or braking, i.e.  $T_M = T_M(\omega_{R_i}, \text{sign}(\dot{\omega}_{R_i}))$ . Within the scope of this paper, we neglect this dependency and, based on measurements of the system at hand, we assume a constant mean time constant of  $T_M \approx 50$  ms, leading to the transfer function

$$\omega_{R_i}(s) = \frac{1}{s \cdot T_M + 1} \omega_{R_i}^{tar}(s) =: G_M(s) \omega_{R_i}^{tar}. \quad (11)$$

Subsequently, each rotor force is obtained by

$$f_i = c_f (G_M(s) \omega_{R_i}^{tar})^2, \quad (12)$$

which, even though the relation is nonlinear, we state by a transfer function for notation convenience. Notice that, in contrast to the the aerodynamic coefficients  $c_f$  and  $c_m$ ,  $T_M$ ,

$c_{u_1}$  and  $c_{u_0}$  can be easily determined with e.g. a photocell, by measuring the rotor speed for different step changes. We ignore these actuator dynamics during the design of the baseline controller and only consider the static relation for control allocation. However, the adaptive part is aimed to perform high adaptation rates so we incorporate the dynamics (11) in the MRAC design.

For the quadrotor at hand, the individual rotor forces are mapped to torques w.r.t each body frame axis and the total thrust  $F_z$  in direction of  $\mathbf{b}_z$  by

$${}^B \begin{pmatrix} \tau_x \\ \tau_y \\ \tau_z \\ F_z \end{pmatrix} = \underbrace{\begin{pmatrix} -l & -l & l & l \\ -l & l & -l & l \\ c_m & -c_m & -c_m & c_m \\ 1 & 1 & 1 & 1 \end{pmatrix}}_M \cdot \underbrace{\begin{pmatrix} f_1 \\ f_2 \\ f_3 \\ f_4 \end{pmatrix}}_f, \quad (13)$$

where  $l$  denotes the lever arm w.r.t. the center of gravity. The control allocation matrix  $M$  has full rank for  $l, c_m > 0$  and thus, is invertible. Individual propeller forces can therefore be obtained from a desired moment and thrust command by the inverse of  $M$ . At this point we have to consider the thrust, even though our focus lies on attitude kinematics, in order to obtain an invertible control allocation matrix. Furthermore, due to saturation of individual propellers, the commanded thrust also has an influence on the obtainable moments, c.f. Section III-C.

## III. CONTROL DESIGN AND ANALYSIS

### A. Attitude Tracking Dynamics

The attitude control system has to make the UAV track a two times differentiable desired reference command, i.e. a given desired attitude  $\mathbf{q}_c$  and angular velocity  $\boldsymbol{\omega}_{CT}$ . This reference frame  $\mathcal{C}$  can be obtained by a trajectory generator as a command filter or from a cascaded higher loop controller, as for example a path model predictive controller. As we only deal with unit quaternions in order to describe rigid body rotations, the error quaternion, describing a vector rotation from the  $\mathcal{B}$ -frame to the  $\mathcal{C}$ -frame, can be stated as

$$\mathbf{q}_e := \mathbf{q}_c^{-1} \otimes \mathbf{q} = \bar{\mathbf{q}}_c \otimes \mathbf{q}. \quad (14)$$

The relative angular velocity between the commanded attitude frame and the body reference frame is

$$\boldsymbol{\omega}_{BC} := \boldsymbol{\omega}_{BI} - \boldsymbol{\omega}_{CT}. \quad (15)$$

This relationship is valid in a general vector notation. However, please note that  $\boldsymbol{\omega}_{BI}$  and  $\boldsymbol{\omega}_{CT}$  lie in different tangent spaces. Therefore their components have to be transformed in a common frame before their components may be subtracted. For the error angular velocity the components in the body reference frame follow to be,

$${}^B \boldsymbol{\omega}_{BC} = {}^B \boldsymbol{\omega}_{BI} - \mathbf{R}_{BI} \mathbf{R}_{CI}^\top {}^C \boldsymbol{\omega}_{CT} = {}^B \boldsymbol{\omega} - \mathbf{R}_{BC} {}^C \boldsymbol{\omega}_c. \quad (16)$$

The time derivative of the quaternion error  $\mathbf{q}_e$  follows to be:

$$\begin{aligned}\dot{\mathbf{q}}_e &= \frac{d}{dt}(\bar{\mathbf{q}}_c \otimes \mathbf{q}) = \dot{\bar{\mathbf{q}}}_c \otimes \mathbf{q} + \bar{\mathbf{q}}_c \otimes \dot{\mathbf{q}} \\ &= \frac{1}{2} [-\epsilon({}^c\boldsymbol{\omega}_c) \otimes \mathbf{q}_e + \mathbf{q}_e \otimes \epsilon({}^B\boldsymbol{\omega})] \\ &= \frac{1}{2} \mathbf{q}_e \otimes \epsilon({}^B\boldsymbol{\omega}_{BC}),\end{aligned}\quad (17)$$

where the commanded angular velocity is mapped into the body frame via (3). By applying (9) to (15), the time derivative of the tracking error of the angular velocity w.r.t. the  $\mathcal{B}$ -frame gives in general vector notation

$$\frac{d}{dt}({}^B\boldsymbol{\omega}_{BC}) = \frac{d}{dt}(\boldsymbol{\omega}) - \frac{d}{dt}({}^c\boldsymbol{\omega}_c) - \boldsymbol{\omega}_{BC} \times \boldsymbol{\omega}_c. \quad (18)$$

Expressing the above term in body frame components and inserting (10) yields:

$$\begin{aligned}{}^B\dot{\boldsymbol{\omega}}_{BC} &= {}^B\dot{\boldsymbol{\omega}} - \mathbf{R}_{BC} {}^c\dot{\boldsymbol{\omega}}_c - {}^B\boldsymbol{\omega} \times \mathbf{R}_{BC} {}^c\boldsymbol{\omega}_c \\ &= -\mathbf{J}^{-1}[\boldsymbol{\omega}]_{\times} {}^B\mathbf{J}\boldsymbol{\omega} + \mathbf{J}^{-1}\boldsymbol{\tau}_{ext} - {}^B\dot{\boldsymbol{\omega}}_c - [\boldsymbol{\omega}]_{\times} {}^B\boldsymbol{\omega}_c.\end{aligned}\quad (19)$$

### B. Trajectory generator

The purpose of the trajectory generator is to generate from a piece-wise continuous reference signal  $\mathbf{q}_r(t)$  one at least two times differentiable reference command  $\mathbf{q}_c(t)$ , which is subject to bandwidth constraints and which is subsequently passed to the attitude controller. Thereby, reference command following and disturbance rejection behavior of the closed loop system can be decoupled, leading to a two degrees of freedom control design. Starting point of the synthesis are the equations (7) for  $\dot{\mathbf{q}}_c$  and  $\dot{\boldsymbol{\omega}}_c = \mathbf{u}_c$ . Given the difference between the reference and command frame  $\mathbf{q}_{\mathcal{RC}} = \bar{\mathbf{q}}_r \otimes \mathbf{q}_c$ , consider

$$\mathbf{u}_c = -2\omega_0^2 \log_v(\bar{\mathbf{q}}_r \otimes \mathbf{q}_c)^+ - 2D\omega_0\boldsymbol{\omega}_c, \quad (20)$$

with the positive control parameters  $\omega_0, D \in \mathbb{R}^+$ . It can be easily verified with the Lyapunov function  $V = 2\omega_0^2 \langle \log(\mathbf{q}_{\mathcal{RC}}^+), \log(\mathbf{q}_{\mathcal{RC}}^+) \rangle + \frac{1}{2} \boldsymbol{\omega}_c^T \boldsymbol{\omega}_c$  that the proposed system is stable and by applying LaSalle's theorem, that (20) leads to asymptotic *set point stabilization*, c.f. the arguments of III-B. However, one can not conclude asymptotic tracking of  $\mathbf{q}_r$  as LaSalle's theorem is not applicable for time-varying systems. Further more, if an eigenaxis rotation is performed, (20) leads to linear dynamics in the exponential coordinates  $\boldsymbol{\alpha} := \log_v(\bar{\mathbf{q}}_r \otimes \mathbf{q}_c)$  given by

$$\ddot{\boldsymbol{\alpha}} + 2D\omega_0\dot{\boldsymbol{\alpha}} + \omega_0^2\boldsymbol{\alpha} = \mathbf{0}, \quad (21)$$

since for  $\boldsymbol{\omega} \parallel \log_v \mathbf{q}$ ,  $\frac{d}{dt} \log_v \mathbf{q} = \boldsymbol{\omega}/2$  holds. Therefore, for a rest to rest movement, the proposed dynamics will lead to a trajectory subject to the bandwidth  $\omega_0$  with the assigned damping  $D$  on the geodetic of  $\text{SO}(3)$ .

### C. Control allocation and saturation

By inverting the matrix  $\mathbf{M}$  in (13), command inputs for each individual rotor are computed from a desired actuation moment  $\boldsymbol{\tau}_c$  and total thrust  $F_z$ . Therefore, we will design the attitude control loop for  $\boldsymbol{\tau}_c$  as the plant input. However, the control system at hand will inevitably have to deal with

control saturations during high bandwidth aggressive flight as the maximum rotor speed is limited and thrust inversion is not possible. Instead of simply imposing saturations on each individual rotor, we use the approach of [26] and prioritize the control objectives. Control moments around the body axes  $\mathbf{b}_x$  and  $\mathbf{b}_y$  have the highest priority, the total thrust  $T$  the second, and finally the commanded moment around  $\mathbf{b}_z$  the lowest. We adopt the proposed method to our X-configuration and add an individual lower speed limit for each propeller, to make sure that no motor halts during flight. Finally, let the obtained saturated and prioritized controls be given by the static, nonlinear function

$$(\bar{\boldsymbol{\tau}}_c^T, \bar{F}_z)^T := \mathbf{f}_{\text{sat}}[(\boldsymbol{\tau}_c^T, F_z)^T]. \quad (22)$$

### D. Control Law Synthesis

We separate the control into a baseline controller for the nominal system and an adaptive controller to deal with the uncertainties

$$\boldsymbol{\tau}_c = \boldsymbol{\tau}_b + \boldsymbol{\tau}_a. \quad (23)$$

Hereby the adaptive part has only to compensate the deviations of the actual system w.r.t. the nominal system. This approach is more common than a fully adaptive design and leads to a more robust and performant system behavior [20]. The whole control structure we are about to develop is depicted in Figure 2.

1) *Baseline Controller*: For the design of the baseline controller we make use of the same approach as in III-B. It is well known that for the attitude control problem, due to topological obstructions, no global asymptotic stability can be achieved by means of continuous state feedback [3]. Therefore let us consider the following baseline control law given by

$$\begin{aligned}\boldsymbol{\tau}_b &= [\boldsymbol{\omega}_B]_{\times} {}^B\mathbf{J}_D\boldsymbol{\omega}_B + {}^B\mathbf{J}_D \left( {}^B\dot{\boldsymbol{\omega}}_c + [\boldsymbol{\omega}_B]_{\times} {}^B\boldsymbol{\omega}_c - \right. \\ &\quad \left. - k_q \log_v \mathbf{q}_e^+ - k_\omega \boldsymbol{\omega}_{BC} \right),\end{aligned}\quad (24)$$

with two positive control gains  $k_q, k_\omega > 0$  and  $\mathbf{J}_D$  being the nominal design inertia. Note that it incorporates the discontinuity (5) to prevent unwinding. This control law may be interpreted as a nonlinear dynamic inversion control based on the *exponential parameters*  $\log_v \mathbf{q}_e$  with feed-forward terms and differs substantially from existing approaches for quaternion based quadrotor attitude control in the literature, since it does not distort the natural metric on rotations. Given an at least two times continuous differentiable signal  $\mathbf{q}_c$ , the nominal, i.e.  ${}^B\mathbf{J}_D = {}^B\mathbf{J}$ , *autonomous*, piece-wise continuous closed loop dynamics follow to be:

$$\begin{aligned}\dot{\mathbf{q}}_e &= \frac{1}{2} \mathbf{q}_e \otimes \epsilon({}^B\boldsymbol{\omega}_{BC}) \\ \dot{\boldsymbol{\omega}}_{BC} &= -k_q \log_v \mathbf{q}_e^+ - k_\omega \boldsymbol{\omega}_{BC}.\end{aligned}\quad (25)$$

Consider the continuous, piecewise differentiable, positive definite Lyapunov function defined by  $V : \mathbb{S}^3 \times \mathbb{R}^3 \rightarrow \mathbb{R}_0^+$ ,

$$V = \frac{1}{2} k_q \|\mathbf{q}_e\|_{\text{SO}(3)}^2 + \frac{1}{2} \boldsymbol{\omega}_{BC}^T \boldsymbol{\omega}_{BC}, \quad (26)$$

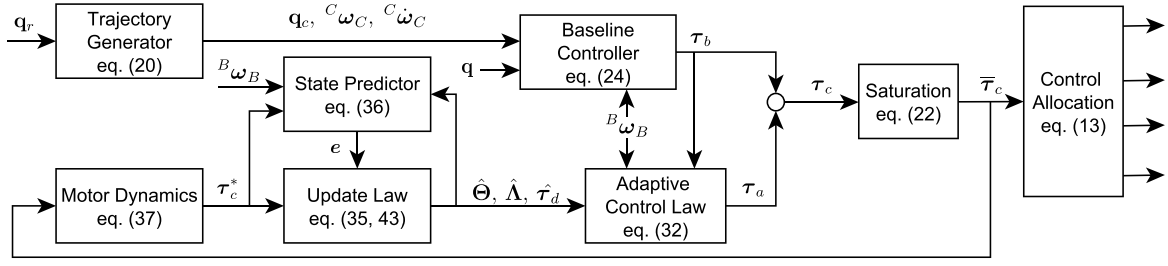


Fig. 2. Overall Controller Structure.

satisfying  $V(\pm \mathbf{q}_{\text{id}}, \mathbf{0}) = 0$ . Its derivative is obtained under consideration of (25) to be  $\dot{V} = -k_\omega \|\omega_{\text{BC}}\|^2 \leq 0$ , which is negative semi definite. Since  $V$  is continuous on the equatorial switching boundary  $S^2$ ,  $\omega_{\text{BC}} \rightarrow \mathbf{0}$  can be concluded. In that case,  $V$  is upper bounded by  $k_q \pi^2/2$ . Thus the trajectories can no longer cross the switching boundary given by  $q_0 = 0$ . Therefore, by invoking LaSalle's invariance principle on the individual hemispheres of  $S^3$ , on which the dynamics of (25) are continuous, global asymptotic stability, in the sense of classical solutions to differential equations, of the set  $\{(\pm \mathbf{q}_{\text{id}}, \mathbf{0})\}$  follows. However, it can be shown that around the switching point a memory-less switching function may not be robust w.r.t. arbitrarily small measurement noise [19] and the authors therefore propose an hysteretic switching instead. As we use a trajectory generator to obtain smooth trajectories with a limited bandwidth, we assume that an attitude error of  $\pi$  does not appear, since the closed loop system is fast enough to follow the desired trajectory with small errors. In addition, the controller is implemented digitally, inheriting a sample and hold behaviour, thus improving the robustness issue around  $q_0 = 0$ .

2) *Adaptive Augmentation*: One of the main uncertainties associated with the system at hand are the parametric values of the inertia tensor  ${}^B \mathbf{J}$  and the control effectiveness, which incorporates the aerodynamic coefficients  $c_f$  and  $c_m$ . Under the common assumption that the body reference frame is a principal axis system, i.e.  ${}^B \mathbf{J} = \text{diag}(J_x, J_y, J_z)$ , the gyroscopic term can be expressed as

$${}^B \mathbf{J}^{-1} [\omega]_{\times} {}^B \mathbf{J} \omega = \begin{pmatrix} \frac{J_z - J_y}{J_x} \omega_z \omega_y \\ \frac{J_x - J_z}{J_y} \omega_x \omega_z \\ \frac{J_y - J_x}{J_z} \omega_x \omega_y \end{pmatrix} =: \begin{pmatrix} \theta_1 \omega_z \omega_y \\ \theta_2 \omega_x \omega_z \\ \theta_3 \omega_x \omega_y \end{pmatrix}. \quad (27)$$

The adaptation algorithm will have to deal with uncertainties in  $\theta_i \in \mathbb{R}$  and the control effectiveness. Therefore, we consider the rotational dynamics

$$\dot{\omega}_B = \Theta \Phi(\omega_B) + \Lambda \tau_c + \tau_d, \quad (28)$$

with the unknown control effectiveness matrix  $\Lambda = \text{diag}(\lambda_1, \lambda_2, \lambda_3) \succ 0$ , the unknown parameter matrix  $\Theta = \text{diag}(\theta_1, \theta_2, \theta_3)$ , the known vector of basis functions  $\Phi = -(\omega_z \omega_y, \omega_x \omega_z, \omega_x \omega_y)^\top$  and the unknown constant disturbance  $\tau_d$ , which is no longer a moment but an angular acceleration disturbance. By this definition, the design control effectiveness comes to be  $\Lambda_D = \mathbf{J}_D^{-1}$ . Note that all appearing uncertainties are matched, i.e. they lie in the

image space of the control input  $\tau_c$ . However, the presented approach is not able to handle motor or propeller faults well, since we do not incorporate the information of (13). Please remember, that our goal is performance oriented and not a fault tolerant design. We formulate an indirect adaptive controller for the body rate dynamics which shall restore the nominal design dynamics of (25), which can be expressed in terms of  $\omega_B$  as

$$\dot{\omega}_B^D = \mathbf{A}_m \omega_B^D + r, \quad (29)$$

with the reference signal  $r = k_\omega {}^B \omega_c + {}^B \dot{\omega}_c - k_q \log_v \mathbf{q}_e^+$ . This novel formulation consists the time dependent, nominal system matrix  $\mathbf{A}_m = -k_\omega \mathbf{I} - [{}^B \omega_c]_{\times}$ , which is stable, since it satisfies the Lyapunov equality  $\mathbf{A}_m^\top \mathbf{P} + \mathbf{P} \mathbf{A}_m = -2k_\omega \mathbf{I}$ , for  $\mathbf{P} = \mathbf{I}$ . In contrast to existing approaches, we want the system to track the *time variant* reference dynamics. Thus, based on (29), we define the following *closed loop reference model*

$$\dot{\omega}_B^m = \mathbf{A}_m \omega_B^m + r - k_e e, \quad (30)$$

consisting the tracking error  $e := \omega_B^m - \omega_B$  between the reference and actual angular velocity, which both are part of the same vector space  $T_{\mathbb{R}} \text{SO}(3)$ . The last term parametrized by  $k_e > 0$  leads to improved transient dynamics of the adaptive controller and can be used to largely reduce oscillations [7]. Inserting the baseline controller into (28), the perturbed real dynamics can be reformulated as

$$\dot{\omega}_B = - \left( k_\omega \mathbf{I} + [{}^B \omega_c]_{\times} \right) \omega_B + (\Theta - \Theta_D) \Phi + \Lambda [\tau_a + (\mathbf{I} - \Lambda^{-1} \mathbf{J}_D^{-1} \tau_b)] + \tau_d + r. \quad (31)$$

Choosing the adaptive control law

$$\tau_a = \hat{\Lambda}^{-1} \left[ - \left( \hat{\Theta} - \Theta_D \right) \Phi - \hat{\tau}_d \right] - \left( \mathbf{I} - \hat{\Lambda}^{-1} \mathbf{J}_D^{-1} \right) \tau_b, \quad (32)$$

where  $(\hat{\cdot})$  are the estimates of the unknown parameters, we want to determine the parameter update laws of the estimates. For this purpose, we formulate the tracking error dynamics while neglecting the closed loop augmentation of our reference model, c.f. [7], i.e.  $k_e = 0$ ,

$$\dot{e} = \mathbf{A}_m e + \tilde{\Theta} \Phi + \tilde{\tau}_d + \tilde{\Lambda} \tau_c. \quad (33)$$

This expression contains the estimation errors  $\tilde{\Theta} := \hat{\Theta} - \Theta$ ,  $\tilde{\Lambda} := \hat{\Lambda} - \Lambda$  and  $\tilde{\tau}_d := \hat{\tau}_d - \tau_d$ . By choosing the Lyapunov function

$$V = e^\top \mathbf{P} e + \frac{1}{2} \text{Tr} \left( \tilde{\Lambda} \Gamma_\Lambda^{-1} \tilde{\Lambda}^\top + \tilde{\Theta} \Gamma_\Theta^{-1} \tilde{\Theta}^\top + \gamma_\tau^{-1} \tilde{\tau}_d \tilde{\tau}_d^\top \right), \quad (34)$$

with the gains  $\Gamma_\Lambda^\top = \Gamma_\Lambda \succ 0$ ,  $\Gamma_\Theta^\top = \Gamma_\Theta \succ 0$ ,  $\gamma_\tau > 0$  and calculating its time derivative, one obtains the standard MRAC parameter update laws [10] given by  $\dot{\hat{\Theta}}^\top = -\Gamma_\Theta \Phi e^\top P$ ,  $\dot{\hat{\Lambda}}^\top = -\Gamma_\Lambda u_c e^\top P$  and  $\dot{\hat{\tau}}^\top = -\gamma_\tau e^\top P$ , which render the time derivative negative semi definite,  $\dot{V} = -2k_\omega e^\top I e$ . Therefore all signals and parameter estimates are bounded, i.e. they belong to  $\mathcal{L}_\infty$  and additionally  $\|e\| \in \mathcal{L}_\infty \cap \mathcal{L}_2$  for some arbitrary vector norm. Furthermore,  $\|e\| \rightarrow 0$ , for  $t \rightarrow \infty$ , follows by Barbalat's lemma [10] or by the theorem of LaSalle-Yoshizawa [14]. However, these update laws can be shown to be not robust w.r.t. sensor noise and unmatched or unstructured uncertainties. Thus, we adopt standard robustness modifications, namely parameter projection and  $\epsilon$ -modification to suppress parameter drift in the adaptation, see [10]. The update laws then follow as

$$\begin{aligned} \dot{\hat{\Theta}}^\top &= -\Gamma_\Theta \text{Proj} \left( \hat{\Theta}, \Phi e^\top P - \sigma_\Theta |e| (\hat{\Theta} - \Theta_D) \right) \\ \dot{\hat{\Lambda}}^\top &= -\Gamma_\Lambda \text{Proj} \left( \hat{\Lambda}, \tau_c e^\top P - \sigma_\Lambda |e| (\hat{\Lambda} - \Lambda_D) \right) \\ \dot{\hat{\tau}}^\top &= -\gamma_\tau \text{Proj} \left( \hat{\tau}, e^\top P - \sigma_\tau |e| \hat{\tau} \right) \end{aligned} \quad (35)$$

with  $\sigma_\Theta, \sigma_\Lambda, \sigma_\tau > 0$ . Due to the deviation of the unmodified, ideal update laws, asymptotic stability can no longer be achieved, however the adaptation with robustness modifications leads to uniform ultimate boundedness (UUB) of the tracking error [20].

For implementation, we will further reformulate (30) into a state predictor form, by adding and subtracting  $\hat{\Lambda} \tau_c$  and replacing  $\tau_c$  by (24) and (32), so one obtains

$$\dot{\omega}_B^m = -k_e e + \hat{\Theta} \Phi + \hat{\Lambda} \tau_c + \hat{\tau}_d. \quad (36)$$

Note that this formulation is not possible without the closed reference model modification with  $k_e > 0$  we applied in (30), as it would lead to unstable dynamics. This form allows us to deal easily with control saturation by Pseudo Control Hedging [11]. For this purpose  $\tau_c$  in (36) and (35) is replaced considering (12) and (13) by the effectively achieved control<sup>2</sup>:

$$(\tau_c^{*T}, F_z^*)^T = M_{ki}^{-1} \left( G_M(s) \sqrt{M_{ij}} (\bar{\tau}_c^T, \bar{F}_z^T)^T \right)^2, \quad (37)$$

which considers the saturations from III-C and motor dynamics. Thus, the reference model and subsequently the adaptation are protected from the nonlinearities in the control channel.

3) *Gyroscopic cross coupling*: In the following, we will have a closer look at the parameter  $\Theta$ , describing the gyroscopic cross coupling of a rigid tumbling body. To our best knowledge, these parameter are assumed to be independent from each other, in the literature dealing with adaptive attitude control. However, only an open subset of  $\mathbb{R}^3$  can occur as tuples  $(\theta_1, \theta_2, \theta_3)$  in real physical systems. With the variables  $\beta_x = \int x^2 dV$ ,  $\beta_y = \int y^2 dV$ ,  $\beta_z = \int z^2 dV$  and under consideration that  $J_x = \int y^2 + z^2 dV$ ,

<sup>2</sup>Again, we use - strictly speaking illegal - the transfer function for short notation. Einstein's summation convention is applied.

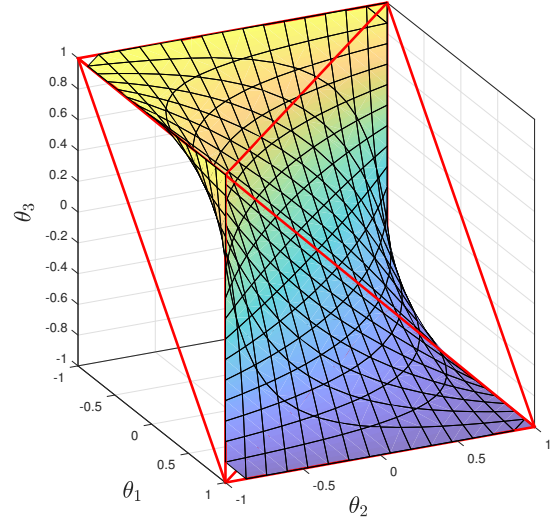


Fig. 3. Physically feasible values of  $\theta_i$  given by the smelt petal  $\Sigma$  and the edges of its convex hull polytope  $\Sigma_c$  (red).

$J_y = \int x^2 + z^2 dV$  and  $J_z = \int x^2 + y^2 dV$  it follows that

$$\theta_1 = \frac{\beta_y - \beta_z}{\beta_y + \beta_z}, \quad \theta_2 = \frac{\beta_z - \beta_x}{\beta_x + \beta_z}, \quad \theta_3 = \frac{\beta_x - \beta_y}{\beta_x + \beta_y}. \quad (38)$$

The physical constraints  $\beta_x, \beta_y, \beta_z > 0$  therefore lead to the well known boundaries  $|\theta_1| < 1$ ,  $|\theta_2| < 1$ ,  $|\theta_3| < 1$ , which give a first bound for the projection of  $\Theta$  in (35) to limit the estimated parameters to physically plausible values. Equation (27) on the other hand can be reformulated as

$$\begin{pmatrix} \theta_1 & 1 & -1 \\ -1 & \theta_2 & 1 \\ 1 & -1 & \theta_3 \end{pmatrix} \begin{pmatrix} J_x \\ J_y \\ J_z \end{pmatrix} = \mathbf{0}, \quad (39)$$

which has a non trivial solution if and only if the above matrix is singular, leading to the following implicit function:

$$F(\Theta) := \theta_1 \theta_2 \theta_3 + \theta_1 + \theta_2 + \theta_3 = 0 \quad (40)$$

Note, that the case of a fully axis-symmetric rigid body corresponds to  $\theta_i = 0$ . Figure 3 depicts the resulting two dimensional manifold, which is called the *smelt petal* [22], given by

$$\Sigma := \left\{ (\theta_1, \theta_2, \theta_3) \in \mathbb{R}^3 \mid F = 0, |\theta_i| < 1 \right\}. \quad (41)$$

An adaptive control algorithm should guarantee, that the estimated parameters are part of the manifold  $\Sigma$ . The convex hull  $\Sigma_c := \text{conv } \Sigma$  can be directly used in the projection modification of equation (35). Additionally, the normal unit vector  $n$  to the surface  $F(\Theta) = c$  denotes

$$n(\Theta) := \frac{\text{grad } F}{\|\text{grad } F\|} \Big|_{\Theta}. \quad (42)$$

Therefore, consider the following modification leading to the novel parameter update law

$$\begin{aligned} \dot{\hat{\Theta}}^\top &= -\Gamma_\Theta \text{Proj} \left( \hat{\Theta}, \Phi e^\top P - \right. \\ &\quad \left. - \sigma_\Theta |e| (\hat{\Theta} - \Theta_D) - k_F F(\hat{\Theta}) n(\hat{\Theta}) \right). \end{aligned} \quad (43)$$

With a constant design parameter  $k_F > 0$ , the estimate  $\hat{\Theta}$  is pulled towards  $\Sigma$ . Especially during phases with low excitation this amendment improves the estimation capabilities and reduces parameter drift. From a Lyapunov perspective, the uniform ultimate boundedness property of the tracking error is still valid, as all quantities  $k_F$ ,  $F(\hat{\Theta})$  and  $\hat{\Theta}^T \mathbf{n}$  are finitely upper bounded in the cube  $-1 < \theta_i < 1$ , or respectively  $\Sigma_c$ .

#### IV. EXPERIMENTAL RESULTS

##### A. Hardware

The test equipment consists of a small custom designed, proprietary quadrotor UAV, which is depicted in Figure 1. Its diagonal has a length of 350 mm from rotor to rotor and the overall mass is 0.8 kg. The flight controller is implemented on a Texas Instruments F28377S Launchpad [9], which is connected to a small consumer grade, low-cost MEMS IMU. Both the data fusion and the control algorithm loop run with 1 kHz, allowing high bandwidth flight maneuvers. Data fusion is performed by a custom nonlinear quaternion based complementary filter with bias estimation for the angular rates, delivering high-quality state estimates for the attitude control. Telemetry data is sent to a ground computer by a rate of 200 Hz via WiFi.

##### B. Flight Test

As a real world validation of the proposed attitude controller we present two case studies. The first flight test demonstrates an unperturbed scenario of the nominal system. However, the parameter of the UAV have been only roughly estimated, based on similar configurations. During the flight, a human pilot commands the height and the reference attitude to the quadrotor. In addition, automated pulses can be generated for the roll reference. The recorded attitude data is depicted in Fig. 4, showing the desired (red) and achieved (blue) Euler angles. At the instant of time marked by the dashed red line, the adaptive augmentation is switched on. It can be observed that, the baseline controller, even though it stabilizes the system, does not perform satisfactory since large overshoots occur, due to the uncertainty. In contrast, the nominal system behavior is mostly restored by the adaptive augmentation. A close up of the roll angle, which is depicted in Fig. 5, shows the response of the quadrotor to two subsequent 350 ms step inputs of 20 degrees height with different signs. With the adaptive augmentation, the quadrotor is able to follow the generated trajectory with high precision even during fast transients and achieves its set point in less than 0.2 s.

For the second flight test, an eccentric mass of approximately 80 g has been attached to the right arm tip in the front of the quadrotor, causing the baseline controller to exhibit a large offset in pitch and roll and thus, it is not able to track the desired attitude, c.f. Fig. 6. The tracking error is effectively diminished by the adaptive augmentation and the performance of the design system is restored, c.f. Figure 7. In contrast to simple integral control to deal with attitude offsets, the performance is not affected and no oscillatory behaviour is introduced. Thus, the controller is able to deal

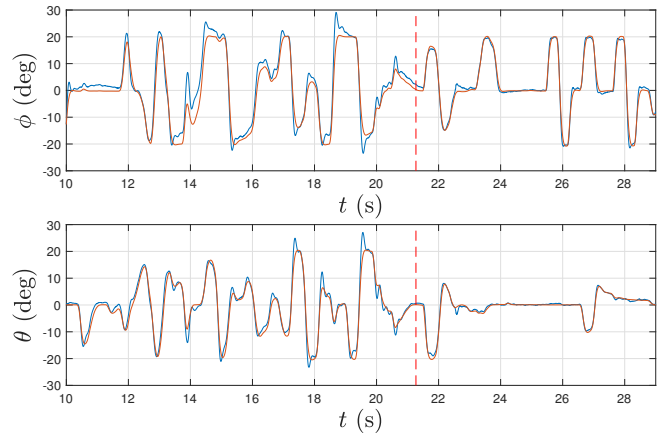


Fig. 4. Flight test 1: Roll and pitch angle from IMU (blue) and from the trajectory generator (red).

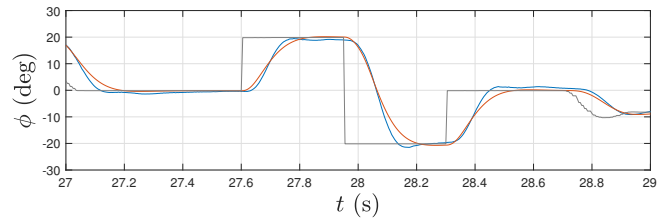


Fig. 5. Flight test 1: Roll angle from IMU (blue), roll angle from the trajectory generator (red) and reference command (grey).

with variable payload or payload distribution, eliminating the need of cumbersome control parameter reconfiguration and tuning. A video, showing the flight performance of the UAV, can be found at:

<https://youtu.be/zK0lp6j6C-I>

#### CONCLUSION

A new quaternion based attitude controller has been presented, consisting of a geometrical baseline controller in conjunction with an indirect MRAC augmentation. The novel baseline controller is based on the quaternion logarithm, leading to linear dynamics in the exponential coordinates of the nominal system during rest-to-rest movements. In contrast to state-of-the-art approaches, a time variant reference model is aimed to be tracked by the adaptive augmentation. In addition, we make use of the special structure of the inertia tensor in our adaptive design and restrict the estimated parameters to physically plausible values. This approach enables fast, aggressive maneuvers, even in the presence of parametric uncertainties, like e.g. payload changes.

Flight tests show the performance capabilities, with very few oscillations and overshoots, even during transients by fast set point changes. Therefore, control implementation is substantially facilitated, since only rough estimates of ranges of the unknown parameter suffice for a superior closed loop performance. The proposed attitude control might serve as an efficient inner loop controller for an upcoming position controller, when a cascaded structure is considered.

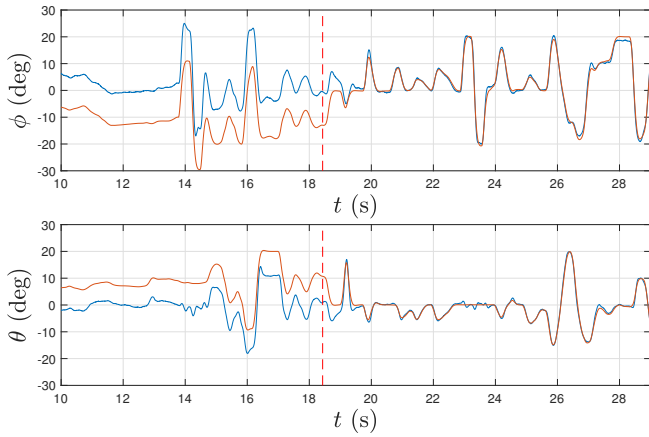


Fig. 6. Flight test 2: Roll and pitch angle from IMU (blue) and from the trajectory generator (red).

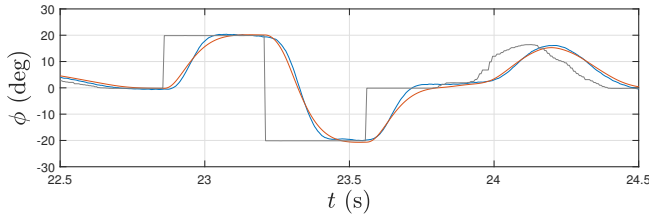


Fig. 7. Flight test 2: Roll angle from IMU (blue), roll angle from the trajectory generator (red) and reference command (grey).

## APPENDIX

### CALCULATION OF THE QUATERNION LOGARITHM

Given the fact that a unit quaternion can be expressed as  $\mathbf{q} = (\cos \alpha/2, \sin \alpha/2 \mathbf{n}^T)^T$ , the logarithm of a quaternion can be computed by

$$\log_v \mathbf{q} = \text{atan2}(\|\boldsymbol{\epsilon}\|, q_0) \frac{\boldsymbol{\epsilon}}{\|\boldsymbol{\epsilon}\|}, \quad (44)$$

which features a singularity at  $\boldsymbol{\epsilon} = \mathbf{0}$ . If we restrict the argument of the logarithm to quaternions with a positive real part, e.g. by passing  $\mathbf{q}^+$ , the atan2 function can be replaced by the regular arctan function. Given the Taylor expansion around zero, it is possible to obtain different degrees of approximation by truncating the series

$$\arctan x = x - \frac{x^3}{3} + \frac{x^5}{5} - \frac{x^7}{7} + \dots \quad (45)$$

Thus, for small rotation angles, a singularity free method to calculate the quaternion logarithm around  $\mathbf{q}_{id}$  denotes:

$$\log_v \mathbf{q} = \frac{\boldsymbol{\epsilon}}{q_0} \left[ 1 - \frac{\|\boldsymbol{\epsilon}\|^2}{3q_0^2} + \frac{\|\boldsymbol{\epsilon}\|^4}{5q_0^4} - \frac{\|\boldsymbol{\epsilon}\|^6}{7q_0^6} + \dots \right]. \quad (46)$$

## REFERENCES

- [1] M. Achtelik, T. Bierling, J. Wang, L. Höcht, and F. Holzapfel. Adaptive control of a quadcopter in the presence of large/complete parameter uncertainties. In *Infotech@Aerospace 2011*, AIAA, 2011.
- [2] V. S. Akkinapalli, G. P. Falconi, and F. Holzapfel. Attitude control of a multicopter using augmented quaternion based backstepping. In *2014 IEEE International Conference on Aerospace Electronics and Remote Sensing Technology*, pages 170–178, Nov 2014.

- [3] S. P. Bhat and D. S. Bernstein. A topological obstruction to continuous global stabilization of rotational motion and the unwinding phenomenon. *Systems & Control Letters*, 39(1):63 – 70, 2000.
- [4] S. Bouabdallah, A. Noth, and R. Siegwart. Pid vs lq control techniques applied to an indoor micro quadrotor. In *2004 IEEE/RSJ International Conference on Intelligent Robots and Systems (IROS)*, volume 3, pages 2451–2456 vol.3, Sept 2004.
- [5] F. Bullo and R. M. Murray. Proportional derivative (PD) control on the Euclidean group. In *European Control Conference*, pages 1091–1097, 1995.
- [6] Z. T. Dydek, A. M. Annaswamy, and E. Lavretsky. Adaptive control of quadrotor uavs: A design trade study with flight evaluations. *IEEE Transactions on Control Systems Technology*, 21(4):1400–1406, 2013.
- [7] T. E. Gibson, A. M. Annaswamy, and E. Lavretsky. On adaptive control with closed-loop reference models: Transients, oscillations, and peaking. *IEEE Access*, 1:703–717, 2013.
- [8] D. Q. Huynh. Metrics for 3d rotations: Comparison and analysis. *Journal of Mathematical Imaging and Vision*, 35(2):155–164, 2009.
- [9] Texas Instruments. C2000 Delfino MCUs F28377S LaunchPad Development Kit. <http://www.ti.com/tool/LAUNCHXL-F28377S>, accessed 2018-09-10.
- [10] P. Ioannou and J. Sun. *Robust Adaptive Control*. Prentice-Hall, Inc., Upper Saddle River, NJ, USA, 1995.
- [11] E. N. Johnson and A. J. Calise. Pseudo-control hedging: A new method for adaptive control. In *Advances in Navigation Guidance and Control Technology Workshop*, Alabama, USA, 2000.
- [12] N. B. Knoebel and T. W. McLain. Adaptive quaternion control of a miniature tailsitter uav. In *2008 American Control Conference*, pages 2340–2345, June 2008.
- [13] R. Kristiansen, P. J. Nicklasson, and J. T. Gravdahl. Satellite attitude control by quaternion-based backstepping. *IEEE Transactions on Control Systems Technology*, 17(1):227–232, 2009.
- [14] M. Krstic, P. Kokotovic, and I. Kanellakopoulos. *Nonlinear and Adaptive Control Design*. John Wiley & Sons, Inc., New York, NY, USA, 1st edition, 1995.
- [15] D. Lee, H. Jin Kim, and S. Sastry. Feedback linearization vs. adaptive sliding mode control for a quadrotor helicopter. *International Journal of Control, Automation and Systems*, 7(3):419–428, Jun 2009.
- [16] T. Lee. Robust adaptive attitude tracking on so(3) with an application to a quadrotor uav. *IEEE Transactions on Control Systems Technology*, 21(5):1924–1930, Sept 2013.
- [17] G. Loianno, C. Brunner, G. McGrath, and V. Kumar. Estimation, control, and planning for aggressive flight with a small quadrotor with a single camera and imu. *IEEE Robotics and Automation Letters*, 2(2):404–411, April 2017.
- [18] T. Madani and A. Benallegue. Control of a quadrotor mini-helicopter via full state backstepping technique. In *Proceedings of the 45th IEEE Conference on Decision and Control*, pages 1515–1520, Dec 2006.
- [19] C. G. Mayhew, R. G. Sanfelice, and A. R. Teel. On path-lifting mechanisms and unwinding in quaternion-based attitude control. *IEEE Transactions on Automatic Control*, 58(5):1179–1191, May 2013.
- [20] N. T. Nguyen. *Model-Reference Adaptive Control*. Springer, 2018.
- [21] T. Raffler, J. Wang, and F. Holzapfel. Path generation and control for unmanned multirotor vehicles using nonlinear dynamic inversion and pseudo control hedging. *IFAC Proceedings Volumes*, 46(19):194 – 199, 2013. 19th IFAC Symposium on Automatic Control in Aerospace.
- [22] F. P. J. Rimbrott. *Introductory Attitude Dynamics*. Springer New York, 1989.
- [23] H. Schaub and J. L. Junkins. *Analytical Mechanics of Space Systems*. AIAA Education Series, Reston, VA, 4th edition, 2018.
- [24] M. Schreier. Modeling and adaptive control of a quadrotor. In *2012 IEEE International Conference on Mechatronics and Automation*, pages 383–390, Aug 2012.
- [25] A. Tayebi and S. McGilvray. Attitude stabilization of a four-rotor aerial robot. In *IEEE Conference on Decision and Control (CDC)*, volume 2, pages 1216–1221, 2004.
- [26] J. Wang, T. Raffler, and F. Holzapfel. Nonlinear position control approaches for quadcopters using a novel state representation. In *AIAA Guidance, Navigation, and Control Conference*, Minneapolis, USA, 2012.
- [27] Y. Yu, S. Yang, M. Wang, C. Li, and Z. Li. High performance full attitude control of a quadrotor on so(3). In *2015 IEEE International Conference on Robotics and Automation (ICRA)*, pages 1698–1703, May 2015.